

Investigation of Spindle Rotation Rate Effects on the Mechanical Behavior of Friction Stir Welded Ti 4Al 2V Alloy

Mohammadreza Aali*,†

*Institute for Polymers and Composites (IPC/i3N), School of Engineering, Department of Polymer Engineering (DEP), University of Minho, Campus of Azurém, Guimarães, 4800-058, Portugal

†Corresponding author : Aali@dep.uminho.pt

(Received November 12, 2019 ; Revised December 3, 2019 ; Accepted January 9, 2020)

Abstract

Nowadays, titanium and its alloys are widely utilized in various industrial parts in such areas as the petrochemical, medical, and automotive industries; However, due to structural considerations, application is problematic in cases of joining. Ti 4Al 2V is a new type of titanium alloy, that in point of structure is near to the α -series, which have many applications in critical conditions (moisture, steam, temperature, etc.). One of the main drawbacks of titanium is the welding of this alloy; however, friction stir welding has been found to be a good method in joining solid materials, especially titanium and its alloys. In this research, the effective parameter of spindle rotational rate has been varied through the process and its effect on the mechanical properties was examined.

Key Words : Titanium, titanium alloy Ti 4Al 2V, Friction stir welding (FSW), Tool rotational rate, Strength and hardness

1. Introduction

For several decades titanium applications are widely used in various industries such as aerospace, petrochemical, medical, and automotive industries; that is essentially because of high corrosion resistance, high-temperature resistance, and wear resistance of titanium¹⁻³. According to this issue, the joining process of titanium and its alloys has great importance and plays a crucial role in the different industries¹. On the other hand, welding of titanium and its alloys with traditional methods creates several problems such as brittle structure, the resistance of high residual stresses and undesirable deformation in welded specimens that are undesirable^{1,3}. Indeed, titanium welding using fusion welding methods is somehow impossible. Therefore, using other welding methods such as solid-state welding, as an alternative approach is necessary, in order to able to utilizing titanium and its alloys as desire shape with optimum properties, and it helps to prevent such problems²⁻⁴.

The Ti 4Al 2V alloy is one of the newest titanium al-

loys, which have been suggested for decades in applications requiring high strength and low to moderate temperatures. In order to control the strength and improve the service conditions of this type of alloy joints in various fields, such as marine and nuclear industries and building steam turbine components the need to recognize mechanical properties and the processes of joining and producing structures of the same materials is more evident than before. The high reactivity of titanium alloys has caused many problems against its welding which has reduced their weldability. In other words, the rapid dissolution of oxygen, hydrogen, and nitrogen at temperatures above 500 °C cause brittleness and loss of mechanical properties of the alloy. The solid-state methods such as friction stir welding (FSW)⁵ are used to improve the weldability of these types of alloys. In this way, the rotational movement of the tool causes heat generation which will result in localized deformation of the cross-section of the joint section³. The thermo-mechanical nature of this type of joint prevents the formation of the defects caused by the thawing-freezing

cycle in fusion welding. In recent years, a lot of research has been carried out on joining these alloys with the FSW method to improve the mechanical properties of the joints. The thermomechanical change performed at the joint causes the microstructural changes³⁾ such as microstructure developments such as recovery or recrystallization that can affect the microstructure in terms of grain size and density of displacements³⁾; therefore, the mechanical properties of the joint will be altered under microstructure changes which are subject to the FSW process parameters³⁾.

FSW is a solid-state joining process in which a non-consumable tool is used to connect two workpieces without the need to reach the melting point. The heat required for the material flow is generated by friction between the rotating tool and the workpiece, which causes the material to soften around the tool. While the tool is moving forward on the track, the workpieces are inter-mixed using the mechanical force that the tool inserts into the workpiece, the soft material around the tool is forged and stuck onto the workpieces^{6,7)}. In the butt welding, the shoulder to the point of contact with the surface of the workpiece plunges into the joint zone of the two pieces and after passing the stop time, it starts to move and leads to join.

By a linear movement of the tool on the joining line, the deformed material is transferred from the advancing side (AS) to the retreating side (RS) of the pin, and is forged by the shoulder, resulting in a solid-state joining between two workpieces⁸⁾. This severe plastic deformation in the weld zone leads to a general change in microstructural and, subsequently, in mechanical properties. Fig. 1 shows the advancing side, retreating side and the different areas of the friction stir welding.

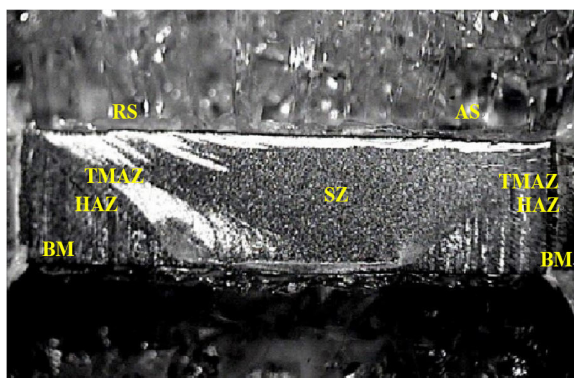


Fig. 1 Micrograph of different signs of substructure zones, Advancing Side (AS), Retreating Side (RS), Stir Zone (SZ), Thermo-Mechanically Affected Zone (TMAZ), Heat-Affected Zone (HAZ), Base Material (BM)

1.1 Friction Stir Welding of Titanium and Its Alloy

Rapp et al.⁹⁾ was one of the first groups to report on the FSW process of titanium with a thickness of 12 [mm] with 17-Ti and Ti 6Al V4 material. Their research included parameter development, metallurgical experiments, mechanical properties, evaluation of post-welding thermal behavior, and assessment of tool materials and heat management of the process. Leinert¹⁰⁾ recently presented a review for the FSW process in which tool material and design, welding parameters, microstructure, hardness and mechanical properties for pure commercial titanium, Beta 21 S, Ti 15V 3Cr 3Al 3Sn, Ti 6Al 4V, and CP Ti is provided. The first experience of Linert et al.¹¹⁾ was the welding of Ti 6Al 4V alloy in which the tool geometry and material and welding parameters were specified¹²⁾. The tool material was pure tungsten with a cylindrical pin of 1.6 [mm] in length, a diameter of 7.9 [mm] and a shoulder diameter of 19 [mm], and the rotation rate parameters of 275 [rpm] and the transverse speed of 100 [mm/min] were used for welding and the temperature of the tool, the microstructure of the weld zone and mechanical properties were investigated. The tool temperature of 1115°C indicated extremely large heat transfer. The microhardness of the weld zone is the same as the base material, but the hardness is increased in the area under the influence of heat. The tensile test indicates a high yield point and tensile strength of the weld zone relative to the base material. Leinert^{10,11)} also referred to the difficulty of choosing a tool for Ti 6Al 4V alloy welding due to high temperatures. For titanium welding, tools with pure tungsten and W-25% Re tungsten-rhenium with HTC have been used successfully. Management methods of thermal activities such as cooling systems are also recommended^{4,12)}.

Lee et al.⁴⁾ studied the FSW microstructure and texture in a 5.6-[mm] thick titanium plate using the FSW process. They showed that the main deformation mechanism in pure titanium happens during the welding process at the same time. In late 2007, the microstructure and hardness of the various zones formed by the FSW process in pure titanium were studied by Lee et al.⁴⁾. At present, numerous efforts have been made to obtain tools with suitable geometry, dimensions, material, tool tilt relative to the spindle axis, transverse speed and rotation rate for joining and forming with higher mechanical properties.

1.2 Investigating the Effect of Different Parameters on the Friction Stir Welding Mechanism

Zhang et al.^{13,14)} investigated the effects of the tilt an-

gle, tool geometry, tool material, rotation rate and transverse speed in joint titanium workpieces welded by FSW. Titanium pieces with dimensions of $3 \times 55 \times 140$ [mm] were prepared for welding and four tools with a pin height of 2.85 [mm], a pin diameter of 5 [mm] and a shoulder diameter of 18 [mm] was used. Based on the design of the tools and test conditions, the experimental test was carried out in four modes^{13,14}. They conclude that the following parameters highly affect to how to connect and perform the process in a better manner, namely: (i) rotation rate and transverse speed, (ii) tool geometry. With an excessive increase in the rotation speed or excessive decrease in transverse speed the weld zone temperature is increased and causes defects in welding. The rotation rate of 750 to 1500 [rpm] and transverse speed of 35 to 100 [mm/min] are the optimum speeds^{14,15}. In the FSW the tool consisting of a pin and shoulder is preferably non-consumable. Three main tasks of the tool include the creation of local heat, the material flow and the control of the fluidized material during the process. Thus, the FSW tool is undoubtedly a major factor in improving this process because it improves the mechanical performance of the joint and obtaining maximum speed of the process¹⁴.

The mechanical deformation and frictional heating of the workpiece which are required for the friction stir force are affected by the design of the tool¹⁶. The shoulder is the main cause of heat generation by friction during the process which compresses the flowing material by introducing the pressure on the workpiece surface and prevents it from escaping from the connecting line. When performing the process, the shoulder moves on the separation line of the two materials and leads to plastic deformation of the material in the area, and this action allows the material to be joined without the need for casting process¹⁴.

In recent years, new geometric features have been developed in the design of the FSW tools^{6,17}. Under the influence of many features of the tools, the movement of matter around the shoulder can be different from one tool to another depending on the tool features¹⁸.

The shape, tilt, length, and diameter of the tool are very important parameters in providing the speed and quality of the FSW process¹⁹. The tool material is also an important parameter¹⁴. Given that the FSW process does not have many problems compare to fusion welding, this process is used for welding aluminum and other soft alloys. The FSW tools create high temperatures and severe stress during the process of hard alloys such as steels and titanium. This has made the use of FSW tools for hard alloys expensive with low lifetime^{3,20}.

2. Materials and Methods

This section is about the applied equipment and the test method. First, the material and size of the specimens are provided and then the device used for welding is discussed. Initially, descriptions are provided on the material type (the sample is near to the α -series alloy of titanium), the weight percent of the elements is discussed and the size of the samples, the method of cutting the samples, the geometry of the tool, as well as the specifications of the device are described.

To carry out tests, Ti 4Al 2V sheets are cut into $50 \times 16 \times 4$ [mm] pieces by wire-cut machine and then using the flat grinding machine, all the parts of the pieces are ground; a view of the raw material is presented in Fig. 2 and its chemical composition is provided in Table 1.

First, due to lack of implementing the FSW process on the Ti 4Al 2V alloy, the tool material, and geometry was selected by the trial and error as high-speed steel (HSS) and hot work steel (H13) and square and cylindrical cross-section were chosen for the pin but due to the high heat generated by friction the tools were failed with the entry of the tools into the piece and temperature increased by friction. Then, using the papers on Ti 6Al 4V alloy FSW the tungsten carbide was used for tool construction. Using the spark machining, a cone-shaped pin has been created. In various papers, the shape and angle of the shoulder for different materials, such as austenitic stainless steels and various titanium alloys are used as concave shapes and at angles of 1 to 6 degrees. In this study using the trial and error test, it was found that the best shape of the shoulder for FSW of Ti 4Al 2V alloy is the concave shoulder and the best

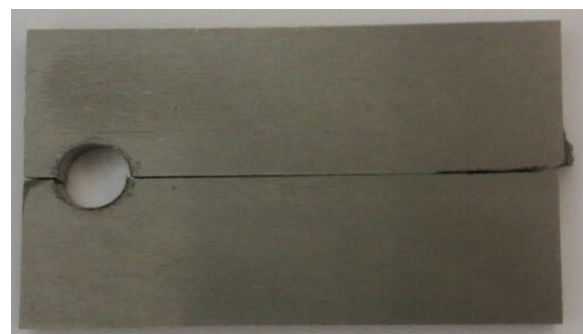


Fig. 2 Scheme of the raw sample was prepared for welding. It was made by two rectangular specimens with $50 \times 16 \times 4$ [mm] dimensions

Table 1 Chemical composition of samples the Ti 4Al 2V

Alloy element	Al	V	Fe	Si	O	N	H	C	Ti
Weight percent	4.05	1.89	0.25	0.12	0.15	0.04	0.01	0.01	balance

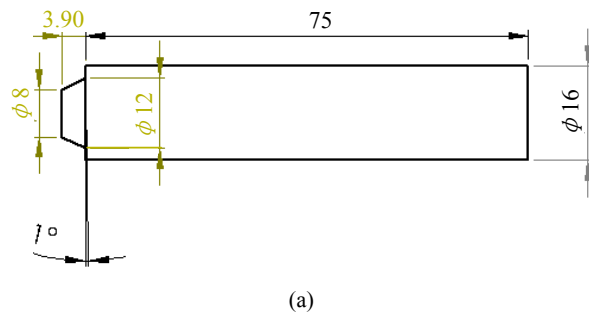


Fig. 3 Geometry of used tool during the process, (a) drawing of the tool, (b) shape of the real tool

shoulder angle is 1 degree. The drawing of used tools during the process and made one is shown in Fig. 3 (all the dimension's units are [mm]).

2.1 Welding Process

The universal milling machine is used to join the pieces by FSW that the tool is mounted on it different fonts. After conducting several studies on the transverse speed of the tool in FSW of titanium; it was found that the transverse speed of 50-100 [mm/min] is within the recommended range for this process. Then, three transverse speeds of 50, 80 and 100 [mm/min] were tested at the same rotational speed and a transverse speed of 100 [mm/min] that the best type of connection was formed at this speed, and it was considered as the constant transverse speed during the process for all samples. The rotation rate of FSW is shown in Table 2. First, a pilot

Table 2 Rotation rate of each sample

Sample No	Rotation rate (rpm)
Sample 1	450
Sample 2	560
Sample 3	710
Sample 4	900
Sample 5	1120

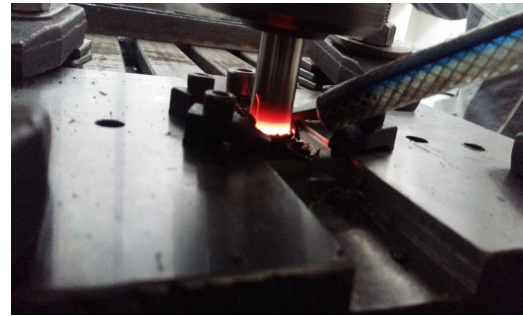


Fig. 4 A perspective view of the FSW during the processing

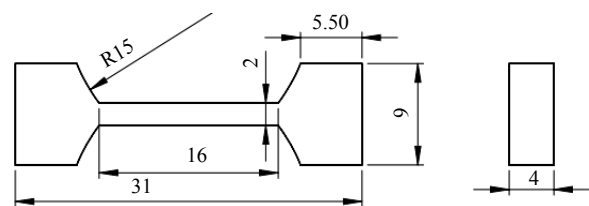


Fig. 5 Tensile test samples scheme

hole with a diameter of 9.8 [mm] has been created to prevent excessive heat rise due to friction and to achieve a pseudo-steady state. The pilot hole diameter is selected completely empirically and based on the pin diameter. The tool tilt compared to the surface of the pieces is one degree. The tool moves to the right. During the welding process, argon gas with a volumetric flow rate of 20 [mL/min] is used to prevent the oxidation of the mixing chamber by reducing the input oxygen pressure and cooling of the tool. Fig. 4 shows a view of the processing condition. Tensile test samples due to the constraints on the dimensions of the pieces are considered as sub-size for the tensile test using a wire cut according to the terms of JIS Z 2241 standard. The prepared sample drawing is presented in Fig. 5 (all the dimension's units are [mm]). The tensile test is carried out transversely with a GOTECH 2-ton traction device.

The metallographic samples are based on the ASTM E3-11 standard, the micro etching of ASTM E 407-2015 and optical microscopy images Leitz (Metallux 3), according to ISO TEC17025 standard. Kroll solution is used for etching the surfaces of the samples. The chemical composition of the Kroll etch soluble consists of 2 [cc] of hydrogen sulfide, 3 [cc] of nitric acid and 500 [cc] of water. Microhardness test is conducted with a force of 300 grams of Vickers and based on the ASTM E384-2016 standard using a Buhler microscope manufactured by the United States on the SZ with a pause of 10 to 15 seconds per hardness testing in a laboratory. The distance between the hardness testing points from each other is three times greater than the diameter of the effect point created by the devise gauge on the material. Moreover, the scanning electron micro-

scope is VEGA\\TESCAN-LMU. The scanning electron microscopy (SEM) is used for fractography of the fracture surfaces of the weld zones in the tensile test.

3. Results and discussion

As explained, the heat generated by the friction force between the tool and the pieces and deformation resulting from it causes the base metal to flow without reaching the melting point and allows the tool to move at the intersection and create the required connection by FSW. Due to the counterclockwise rotation of the tool, the material flow is from the right of the sample (AS) to the left of the sample (RS) which is clearly visible in Fig. 6, and the forging of the flowing materials in the back of the tool is done by the shoulder and created a solid-state junction between the pieces. Due to the plastic deformation in the weld zone, the mechanical properties of the material are changed after welding.

3.1 Examining the Appearance of Weld

As discussed earlier, the samples were joined by FSW using five different rotation rates. In general, the surface of the samples that have been rotated with high speed is much more uniform than those that are connected at a low rotation rate which suggests that increasing the rotation rate improves the quality of the surface of the weld which is visible in Figs. 6 (a) and 6 (b).

Fig. 6 depicts that samples that are connected at the highest rate have the least flash and the appearance of the welding also indicates the proper connection of the two sides of the metal with each other. As the rate increases, the arches appearing on the welding surface are also close to each other which not only affect the appearance of the weld but also the quality of the weld. The best appearance of the weld can be seen at the beginning and the middle (from the tool entry point), but the final points of the welds do not have the desired

quality and smoothness. This applies to all welding cases so that the exit point of the tool (or the electrode in other welds) is always the weakest part because the lack of material at the final point and the heat transfer causes the microstructure to change and sometimes burning the weld zone.

Fig. 7 (a) and 7 (b) show the macroscopic image of the welded cross-section of samples 1 and 2, respectively. In sample 1, due to the rotation rate and transverse speed, it can be concluded that the lack of complete connection due to inadequate heat input has occurred, which is due to the lack of fit between the rotation rate and transverse speed. This defect can be seen with increasing the rotation rate in sample 2 as a pitting; due to the improvement of the conditions in later samples, it can be concluded that the rotation rate of 450 [rpm] and the transverse speed of 100 [mm/min] is high. In specimens 3 and 4, due to the suitability of the rotation rate and transverse speed, no defect is caused (Fig. 7 (c) and Fig. 7 (d)). In Fig. 7 (e), which is related to the sample 5, a fine pitting is observed which indicates that the rotation rate is much higher than the transverse speed.

3.2 Metallography

Fig. 8 shows the microstructure of the base material. The microstructure of the base material is coarse-grained and serrated α -phase (bright) and the grain border is dark. Fig. 9 shows the microstructure of the heat-affected zone of the specimens 1 to 5 which is coarse-grained and serrated, and no plastic deformation has taken place in this zone. The main microstructural difference between the heat-affected zone and the base material is that the grain boundary in the heat-affected zone is not as clear as the base material. That is because the material in the heat-affected zone does not experience any plastic deformation but the input heat from the welding causes the boundaries to begin to move toward each other and



(a)



(b)

Fig. 6 Welding appearance, (a) welding appearance of the sample joint with 450 [rpm] (minimum rotation rate), (b) welding appearance of the sample joint with 1120 [rpm] (maximum one)

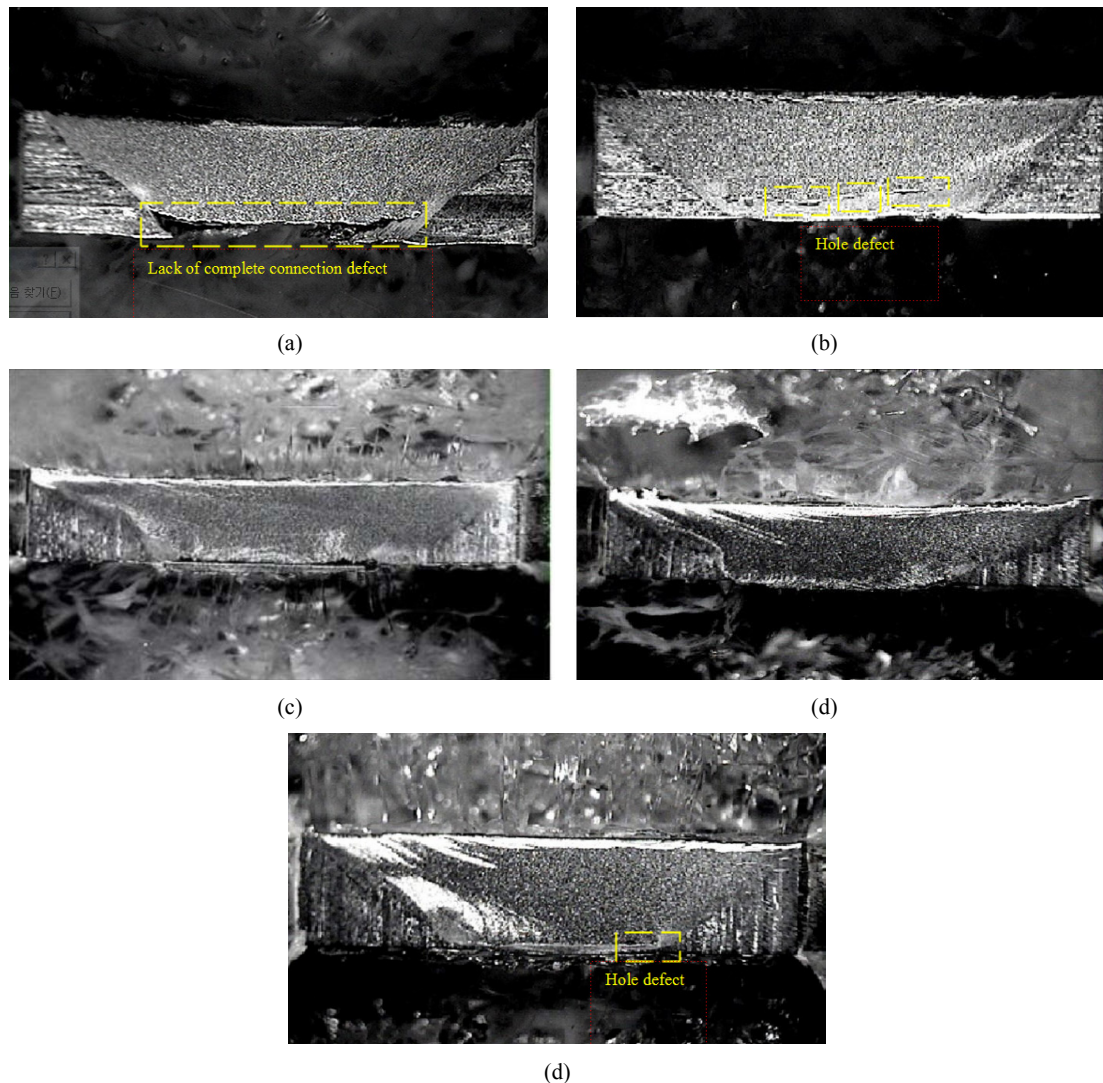


Fig. 7 Macroscopic image of the welded cross-sections, (a) sample 1, (b) sample 2, (c) sample 3, (d) sample 4, (e) sample 5

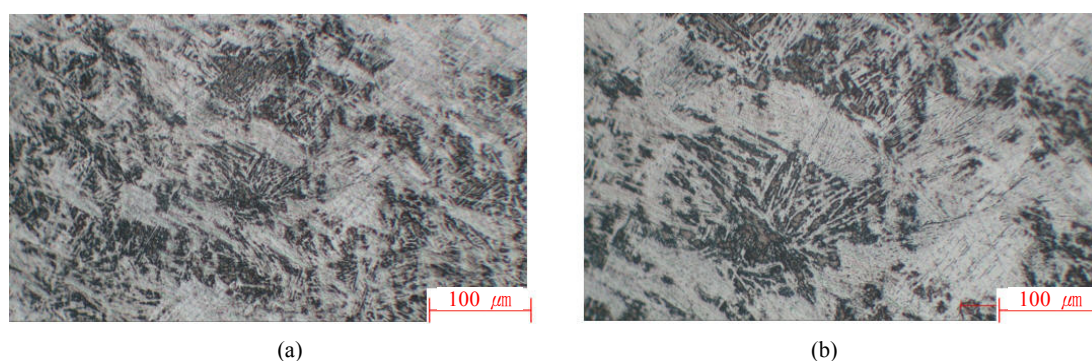


Fig. 8 Microstructure of the base material, (a) 100x magnification; (b) 200x magnification

tend to grow²¹⁾, and there isn't any β -phase neither in grains nor in boundaries. In Fig. 10, the microstructure of the SZ of samples 1 to 5 is observed where the simultaneous effect of the severe plastic deformation and heat generated by the frictional force resulting from the increase of rotation rate during the friction welding

process creates serrated coarse-grain microstructure in this zone.

3.3 Microhardness Test

Fig. 11 shows a schematic view of the welded cross-

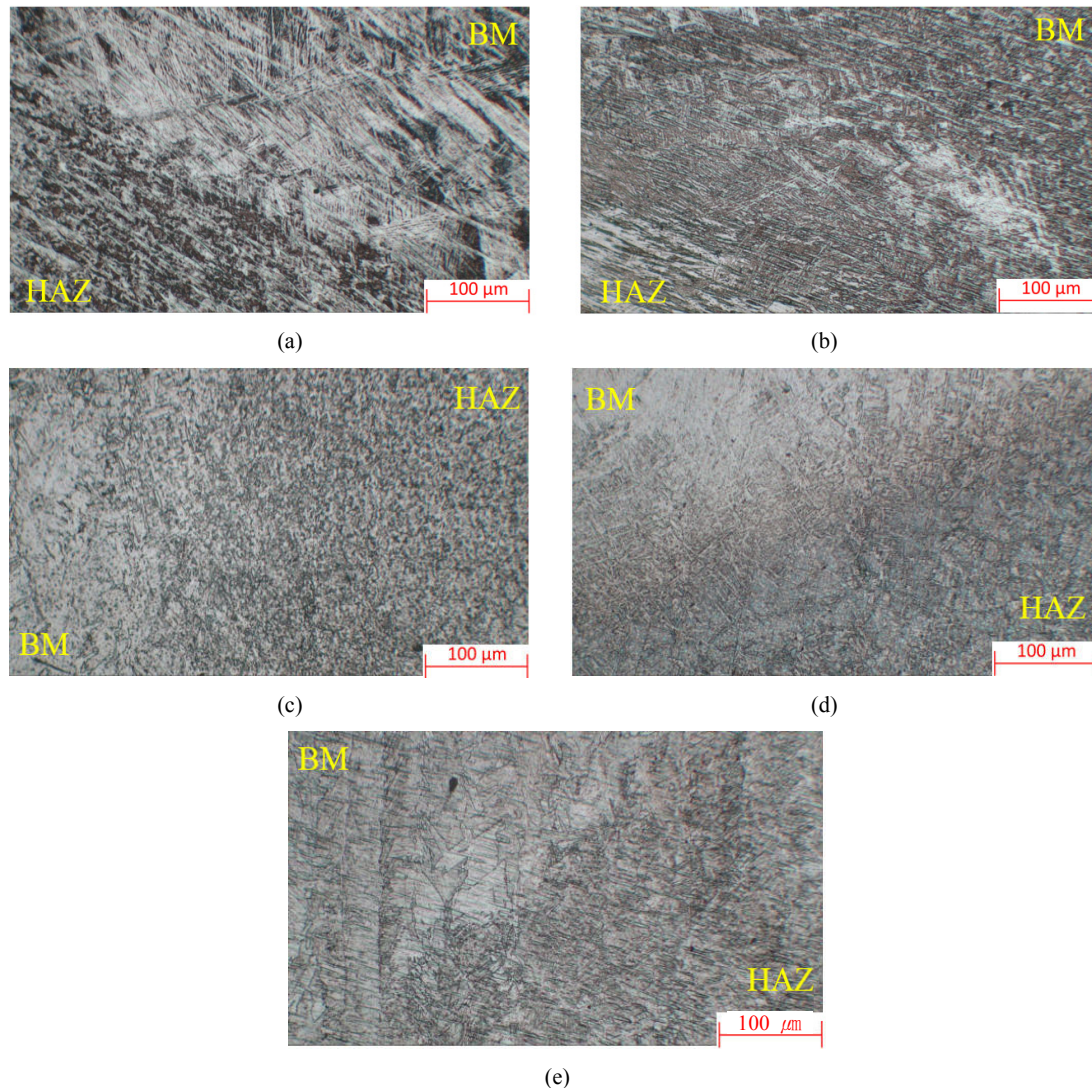


Fig. 9 The substructure of the heat-affected zone: (a) sample 1, (b) sample 2, (c) sample 3, (d) sample 4, (e) sample 5

section. According to the microhardness test results, it can be concluded that with increasing the rotation rate and fixed transverse speed the hardness of the weld zone is increased; however, from the rotation rate of 710 [rpm] (sample 3) on this increase in hardness versus the hardness of the raw material is increased. Due to the lack of observation of the β -phase in the microstructure of the samples after the FSW it can be concluded that the peak welding temperature during the process has not exceeded 882°C which is the titanium deformation point and according to the metallographic results, which indicate a change in the size from the coarse-grain serrated needle shape to the fine-grain serrated needle shape in the SZ, it can be concluded that with increasing rotation rate which increases the friction and temperature in the weld zone a considerable amount of displacement is created by mechanical retention and recrystallization of the grains in the SZ and the displacements can easily move. On the other hand, in the

weld zone, after the FSW a large part of the grains have the same orientation and merely a small part of the has a dissimilar orientation.

Due to changes in the microstructure and high increase in density of displacements, the hardness of the SZ is increased after the FSW.

3.4 Tensile Test

One of the most important welding purposes in metals is to create a higher strength or at least equal to the base metal which can withstand the forces applied to the sample. In all the welds, an attempt is made to increase the strength of the weld above the base metal and prevent fracture in the interface of the base metal. One of the most important tests for measuring weld quality is the tensile test.

The results obtained from the tensile test of the five samples are shown in Table 3. The tensile strength of

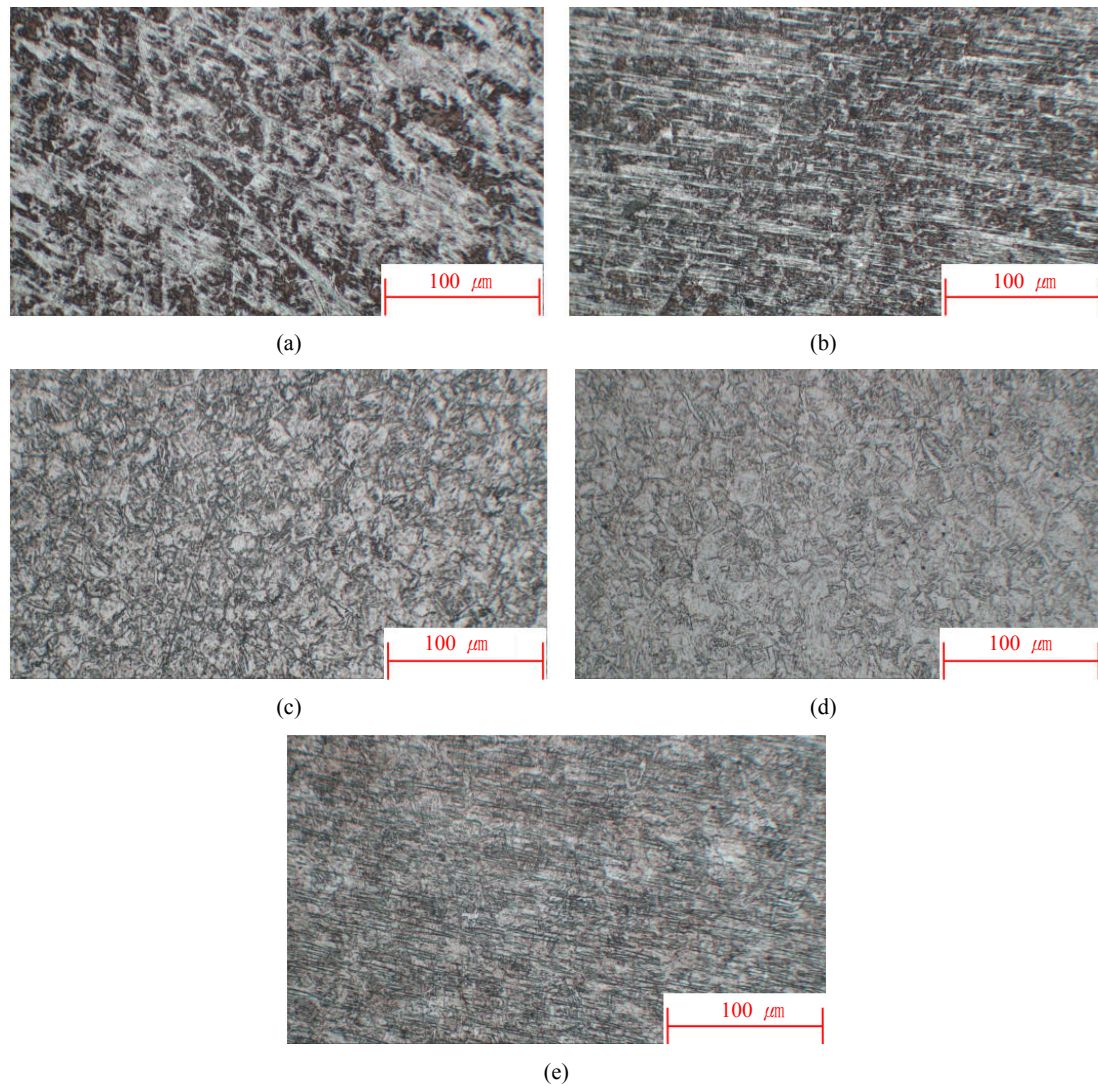


Fig. 10 Microstructure of the stirred zone at the joining line, (a) sample 1, (b) sample 2, (c) sample 3, (d) sample 4, (e) sample 5

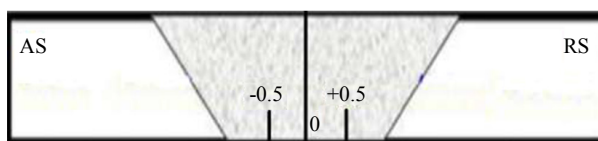


Fig. 11 Schematic view of the cross-section of the welded sample

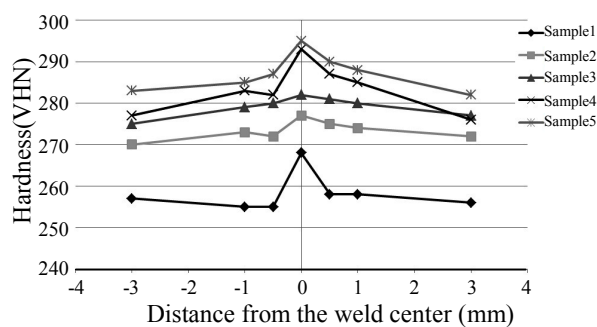


Chart 1 Microhardness test results

Table 3 Tensile test results at the 100 [rpm] transverse speed

Rotation rate (rpm)	450	560	710	900	1120
1 st test Unit (MPa)	589	621	802	560	450
2 nd test Unit (MPa)	564	652	787	599	414

the base material before welding is 700 [MPa]. According to the results obtained from the welded samples, it can be concluded that with increasing rotation rate during welding, the final tensile strength is decreasing. The set of the tensile test samples are shown in Fig. 12. As depicted in Fig. 12 (c), due to the ultimate tensile strength increment in sample 3, the specimen fracture occurred in the raw material zone, and the same has occurred in sample 4 (Fig. 12 (d)). Friction stir welding induces residual stresses to the samples attached by this method which is understandable butt-welded samples

after joining where the sides partially move upward. Enhancement of the rotation rate causes to increase in the temperature in the stir zone. This issue causes a reduction of the residual stress remains in this region. Consequently, the ultimate tensile strength of the sample is reduced^{22,23}.

3.5 Analysis of the Fracture Cross-section

Fig. 13 is the magnified image of the fracture cross-section of samples 1-5 obtained by scanning electron microscopy. In sample 1, according to the fracture cross-section, which is a dimple rupture, it can be

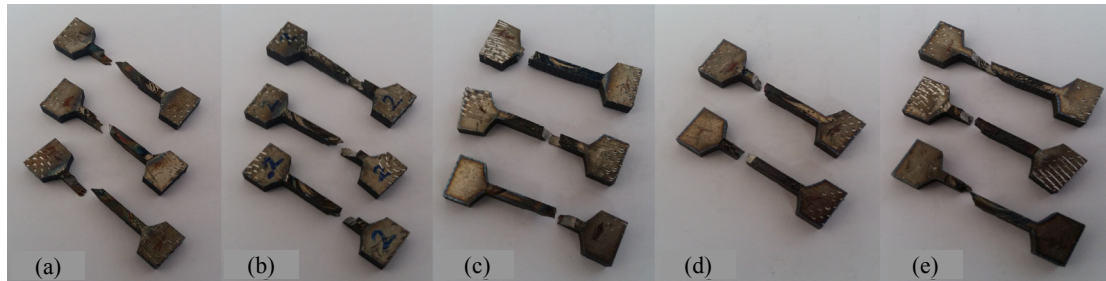


Fig. 12 Set of tensile test samples, (a) sample 1, (b) sample 2, (c) sample 3, (d) sample 4, (e) sample 5

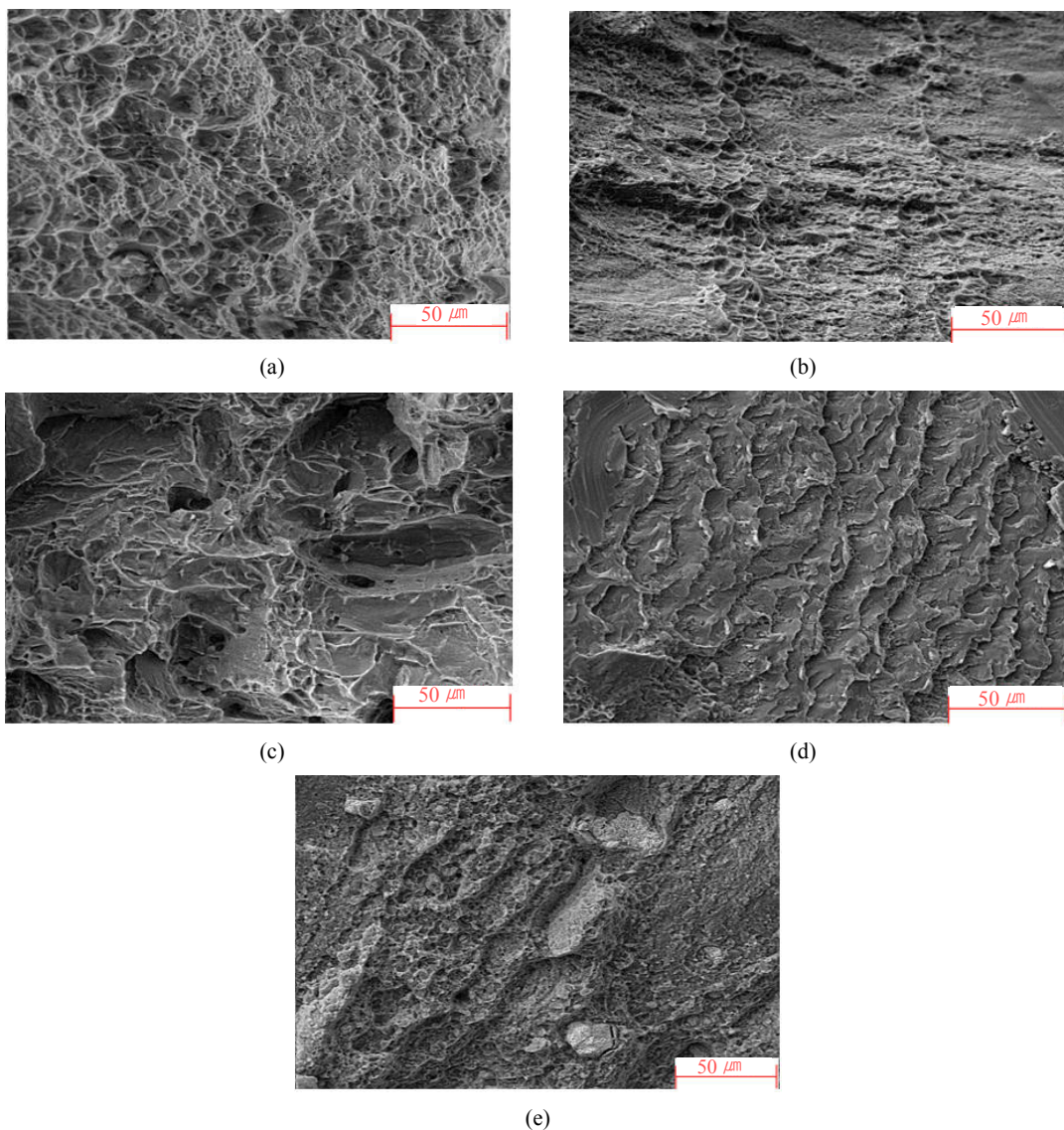


Fig. 13 SEM images of the fracture cross-section of samples, (a) sample 1, (b) sample 2, (c) sample 3, (d) sample 4, (e) sample 5

concluded that the type of fracture occurred in this sample is soft. In sample 2, the depth of the dumbbell caused by the limited micro-plastic deformation is reduced and on the other hand, with the continuation of the dumbbell shape in the lower part of the image, it shows that the micro-mechanism of failure is inclined toward a pseudo cleavage.

In Figs. 13 (c), 13 (d) and 13 (e) of samples 3, 4 and 5, it is seen that the micro-mechanism of dumbbell formation is not a working mechanism, in other words, the microplastic deformation is completely stopped, and on the other hand, the appearance of the mechanism of toroidal plates at the fracture section in micro dimensions indicates the onset and dominance of the cleavage micro-mechanism and the function of the twins is the plastic deformation in titanium alloy which causes a relative increase in the percentage of cleavage in the cross-section. In other words, with the relative increase in hardness, the situation has progressed to cleavage.

4. Summary

1) The lack of coordination between the rotation rate and transverse speed of the tool causes defects such as pitting in the weld zone which is caused by insufficient input heat.

2) With increasing rotation rate the hardness of the weld zone increases compared to the base material.

3) According to the results obtained from the tensile, microhardness and metallography tests, it can be concluded for a transverse speed of 100 [mm/min] the best rotation rate is 710 [rpm].

4) In order to achieve optimal properties at higher rotation rates, the transverse speed should increase proportionally to the rotation rate.

ORCID: Mohammadreza Aali: <http://orcid.org/0000-0003-2075-737X>

References

1. G. Lütjering and J. C. Williams, Titanium. *Springer*, 446, (2007).
<http://doi.org/10.1007/978-3-540-73036-1>
2. M. J. Donachie, Titanium A Technical Guide. 2nd Edition, *ASM International®*, OHIO, USA (2000) 369.
3. M. K. B. Givi and P. Asadi, Advances in Friction-Stir Welding and Processing, *Elsevier Ltd*, (2014) 796.
<https://doi.org/10.1016/C2013-0-16268-X>.
4. W. B. Lee, C. Y. Lee, W. S. Chang, Y. M. Yeon and S. B. Jung, Microstructural investigation of friction stir welded pure titanium, *Mater. Lett.* 59 (2005) 3315-3318.
<https://doi.org/10.1016/J.MATLET.2005.05.064>.
5. C. J. Thomas, W. M. Nicholas, E. D. Needham, J. C. Murch, M. G. Templesmith, and P. Dawes, International Patent Application No. PCT/GB92/02203 and GB Patent Application No. 9125978.8. (1991).
6. R. S. Mishra and Z. Y. Ma, Friction stir welding and processing, *Mater. Sci. Eng.* 50 (2005) 1-78.
<https://doi.org/10.1016/J.MSER.2005.07.001>.
7. R. S. Mishra, P. S. De, and N. Kumar, Friction Stir Welding Configurations and Tool Selection, *Frict. Stir Weld. Processing*, (2014), 95-108,
https://doi.org/10.1007/978-3-319-07043-8_4
8. T. U. Seidel, and A. P. Reynolds, Visualization of the material flow in AA2195 friction-stir welds using a marker insert technique. *Metall. Mater. Trans. A* 32, (2001) 2879-2884.
9. T. Rapp, E. Helder and P. R. Subramanian, FSW of Titanium Alloys for Aircraft Engine Components, *Frict. Stir Weld. Processing II, : Proceedings of the TMS Annual Meeting*, (2003) 173-178.
10. T. J. Lienert, Microstructure and Mechanical Properties of Friction Stir Welded Titanium Alloys, *Frict. Stir Weld. Proces.* (2007) 123-154.
11. T. J. Leinert, K. V. Jata, R. Wheeler, and V. L. Seetharaman, Friction Stir Welding of Ti-6Al-4V Alloys, *Proceedings from Joining of Advanced and Specialty Materials(ASM International)*, St. Louis, MO, (2000).
12. P. Edwards and M. Ramulu, Identification of Process Parameters for Friction Stir Welding Ti-6Al-4V. *J. Eng. Mater. Technol.* 132 (2010) 031006.
<https://doi.org/10.1115/1.4001302>.
13. Y. Zhang, Y. S. Sato, H. Kokawa, S. H. Park and S. Hirano, Stir zone microstructure of commercial purity titanium friction stir welded using pcBN tool, *Mater. Sci. Eng. A* 488 (2008) 25-30.
<https://doi.org/10.1016/j.msea.2007.10.062>
14. Y. Z. Zhang, X. Cao, S. Larose and P. Wanjara, Review of tools for friction stir welding and processing. *Canadian Metall. Q.* 51 (2012) 250-261.
<https://doi.org/10.1179/1879139512Y.00000000015>
15. J. Ding, B. Carter, K. Lawless and J. Schneider, A Decade of Friction Stir Welding R & D At NASA's Marshall Space Flight Center And a Glance into the Future by. *Source Acquis. NASA Marshall Sp. Flight Cent.*, (1994).
16. K. Reshad Seighalani, M. K. Besharati Givi, A. M. Nasiri and P. Bahemmat, Investigations on the Effects of the Tool Material, Geometry, and Tilt Angle on Friction Stir Welding of Pure Titanium, *J. Mater. Eng. Perform.* 19 (2010) 955-962.
<https://doi.org/10.1007/s11665-009-9582-8>
17. R. S. Mishra and M. W. Mahoney, *Friction Stir Welding and Processing*, *ASM International*, (2007).
[https://doi.org/10.1016/S0140-6736\(00\)74398-4](https://doi.org/10.1016/S0140-6736(00)74398-4).
18. M. M. El-Sayed, A.Y. Shash and M. Abd Rabou, Heat Transfer Simulation and Effect of Tool Pin Profile and

- Rotational Speed on Mechanical Properties of Friction Stir Welded AA5083-O. *J. Weld. Join.* 35 (2017) 35-43.
<https://doi.org/10.5781/jwj.2017.35.3.6>.
19. M. M. El-Sayed, A. Y. Shash M. Abd Rabou, Influence of the Welding Speeds and Changing the Tool Pin Profiles on the Friction Stir Welded AA5083-O Joints. *J. Weld. Join.* 35(2017) 44-51.
<https://doi.org/10.5781/jwj.2017.35.3.7>.
20. W. M. Thomas, P. L. Threadgill and E. D. Nicholas, Feasibility of friction stir welding steel. *Sci. Technol. Weld. Join.* 4(1999) 365-372.
<https://doi.org/10.1179/136217199101538012>.
21. W. B. Lee, Y. M. Yeon and Jung, The joint properties of dissimilar formed Al alloys by friction stir welding according to the fixed location of materials, *Scr. Mater.* 49(2003) 423-428.
[https://doi.org/10.1016/S1359-6462\(03\)00301-4](https://doi.org/10.1016/S1359-6462(03)00301-4)
22. M. Aali, Master Thesis, The effect of spindle speed on the Mechanical behavior of friction stir welded Ti 4Al 2V alloy, Azad University, Tabriz, Iran, (2007)
<https://doi.org/10.13140/RG.2.2.19022.20802>.
23. M. Aali and S. J. Azari, Influence of spindle speed on the strength of joint port of Ti 4Al 2V alloy at friction stir welding (FSW). *2nd International Conference on Mechanical Engineering, Industrial and Aerospace*, (2018) 19.